Impurity Band Conduction in a High Temperature Ferromagnetic Semiconductor

K. S. Burch,[1,*] D. B. Shrekenhamer,[1] E. J. Singley,[1,†] J. Stephens,[2] B. L. Sheu,[3] R. K. Kawakami,[2,‡] P. Schiffer,[3] N. Samarth,[3] D. D. Awschalom,[2] and D. N. Basov[1]

[1]*Department of Physics, University of California, San Diego, California 92093-0319, USA*
[2]*Center for Spintronics and Quantum Computation, University of California, Santa Barbara, California 93106, USA*
[3]*Department of Physics and Materials Research Institute, The Pennsylvania State University, University Park, Pennsylvania 16802, USA*

(Received 31 March 2006; published 23 August 2006)

The band structure of a prototypical dilute magnetic semiconductor (DMS), $Ga_{1-x}Mn_xAs$, is studied across the phase diagram via infrared and optical spectroscopy. We prove that the Fermi energy (E_F) resides in a Mn-induced impurity band (IB). Specifically the changes in the frequency dependent optical conductivity [$\sigma_1(\omega)$] with carrier density are only consistent with E_F lying in an IB. Furthermore, the large effective mass (m^*) of the carriers inferred from our analysis of $\sigma_1(\omega)$ supports this conclusion. Our findings demonstrate that the metal to insulator transition in this DMS is qualitatively different from other III-V semiconductors doped with nonmagnetic impurities. We also provide insights into the anomalous transport properties of $Ga_{1-x}Mn_xAs$.

DOI: 10.1103/PhysRevLett.97.087208 PACS numbers: 75.50.Pp, 71.30.+h, 78.30.−j

The dilute magnetic semiconductor $Ga_{1-x}Mn_xAs$ presents a unique opportunity to study carrier mediated magnetism in a well controlled environment. It is generally accepted that the ferromagnetic interaction between the local moments provided by the substitutional Mn (Mn_{Ga}) is mediated by the holes also donated by the Mn_{Ga}, and that for $x < 0.04$ these carriers reside in a Mn-induced impurity band (IB) [1]. However, the nature of the states at higher carrier densities (p), relevant for high ferromagnetic transition temperatures (T_C), remains controversial. It is often assumed that $Ga_{1-x}Mn_xAs$ falls within the Mott picture of the metal to insulator transition (MIT), wherein the IB eventually dissolves into the GaAs valence band (VB). Theoretical studies based on this approach have successfully described some of the properties of $Ga_{1-x}Mn_xAs$ [2,3]. Others have suggested that the persistence of the Mn-induced IB at all carrier densities is critical to describing the physics of $Ga_{1-x}Mn_xAs$ [4–7]. Previous studies have supported the notion that the IB exists in the metallic state at low p [8–12]. Nonetheless, this Letter is the first to conclusively demonstrate the existence of the IB in samples with reduced compensation and defect concentrations revealing the highest reported values of T_C for the concentrations of Mn studied. We also uncover the origin of the small mobility in $Ga_{1-x}Mn_xAs$.

Our determination that E_F lies in an IB is enabled by the distinct free-carrier absorption we observe in highly conductive films, as well as careful analysis of the electromagnetic response of $Ga_{1-x}Mn_xAs$ across its phase diagram. We therefore provide a clear picture of the band structure of $Ga_{1-x}Mn_xAs$ through a detailed spectroscopic study of as-grown and annealed samples. Recently postgrowth annealing has enabled an increase in the T_C and p [13,14]. Annealing achieves this enhancement by removing Mn interstitials (Mn_i) acting as double donors and therefore compensating the holes [15,16]. Consistent with the notion of a boost in p, after annealing the samples we find a large increase in the dissipative part of the optical conductivity [$\sigma_1(\omega)$] for all ω below the band gap of the GaAs host. However, the overall shape of $\sigma_1(\omega)$ in high-T_C ferromagnetic films is remarkably similar to data from an earlier generation of samples [8,10]. The sum-rule analysis of the electronic spectral weight allows us to discern the magnitude of the effective mass of the carriers (m^*), which is much larger than what has been predicted theoretically [2]. Additionally m^* is much larger than what is observed in p-type, nonmagnetic GaAs doped to comparable levels [17], where it is well established that E_F lies in the GaAs VB. Furthermore, we find a significant redshifting of the midinfrared resonance, which is also in direct contradiction to what is observed in p-type, nonmagnetic GaAs [17], and theoretical predications based on E_F lying in the GaAs valence band [2]. However, similar qualitative behavior has been observed in n-type GaAs in the doping regime of a well-defined impurity band [18]. Thus, we establish that the carriers reside in an IB at all values of p. This conclusion is challenging to our current conception of the MIT in a dilute magnetic semiconductor, suggesting an important role for magnetism [19] that had not been previously identified in doped semiconductors.

The samples were grown at UCSB on semi-insulating GaAs (100) by low temperature molecular beam epitaxy and annealed at PSU; see ref. [13] for details. After growth the wafers were split such that optical measurements could be performed on samples from the same growth both before and after annealing. The $Ga_{1-x}Mn_xAs$ layers had a nominal thickness of 40 nm to optimize the increase in T_C upon annealing while still allowing for accurate optical measurements. All samples displayed a well-defined hysteresis loop and T_C when measured with a SQUID magnetometer (see Table I). Room temperature, ellipsometry between 0.62 and 6 eV (5000 → 48 390 cm^{-1}), at 75°

TABLE I. T_C for the four $Ga_{1-x}Mn_xAs$ samples in this study. "A" indicates samples that have been annealed.

x	0.052	0.073	0.052A	0.073A
$T_C(K)$	80	80	120	140

angle of incidence as well as transmission over the range $0.005 \rightarrow 1.42$ eV ($40 \rightarrow 11\,400$ cm^{-1}) from 292 to 7 K were carried out at UCSD. Details of the measurements and extraction of optical constants is described in Refs. [8,9].

We begin with an introduction to the semiclassical Drude-Lorentz model, which provides useful insights into the data. In this model one writes

$$\sigma_1(\omega, x, T) = \frac{\Gamma_D^2 \sigma_{\rm dc}}{\Gamma_D^2 + \omega^2} + \frac{A\omega^2\Gamma_L}{(\Gamma_L\omega)^2 + (\omega^2 - \omega_0^2)^2}, \quad (1)$$

where the first term describes the response of free carriers via the following parameters: Γ_D is the free-carrier scattering rate and $\sigma_{\rm dc}$ is the dc conductivity; the second term describes the interband transition with ω_0 its center frequency, Γ_L its broadening, and A its amplitude. One quantifies the strength of the free-carrier response through the plasma frequency: $\omega_p^2 = \frac{pe^2}{m^*} \cong \frac{2}{\pi}\int_0^\Omega \frac{\Gamma_D^2\sigma_{\rm dc}}{\Gamma_D^2+\omega^2} d\omega$, where e is the charge of the electron and m^* is the effective mass of the carriers [20]. Therefore spectral weight in the far-infrared (FIR) is attributed to the free carriers (intraband response) and is proportional to p divided by m^*. Examples of these shapes are shown on the right side of Fig. 1 via a fit to the 52A data using Eq. (1), wherein the distinct two-component character of the electromagnetic response of annealed samples is uncovered.

On the left side of Fig. 1 we present $\sigma_1(\omega, x, 7\ {\rm K})$ for our new samples along with the spectra from our previous studies [8]. Some absorption is seen in the FIR in all samples, yet a clear Drude feature is seen only in the annealed films. In all of the films a resonance is observed in the midinfrared (MIR) that by itself is consistent with both the VB and IB pictures of the electronic structure. Indeed, if E_F lied in the GaAs VB, then a MIR resonance would result from transitions from the light to heavy hole bands [2]. If, on the other hand, the holes reside in the IB, the MIR resonance results from transitions between the IB and VB [5,8,9]. We can discriminate between these scenarios by increasing p. In particular, the position of the MIR peak should either blueshift or redshift depending on the origin of the transition. A simple diagram of energy versus momentum (k) in Fig. 2 clarifies the rational for this assertion. Panels (a) and (b) assume the Mn-induced IB has dissolved into the VB, where E_F now lies. In panel (a), at low p, an optical transition is realized between the light and heavy hole bands (LH and HH, respectively). When p increases, E_F moves deeper into the valence bands [panel (b)], resulting in an optical transition that shifts to higher energies [2]. If E_F lies in a Mn-induced impurity band (Mn_{Ga}), an optical transition between the LH, HH, and Mn_{Ga} bands will be observed. However, the separation between the IB and the VB is determined, in part, by the Coulomb attraction of the holes to the Mn_{Ga}. Thus as p is increased [panels (c) and (d)], the Coulomb attraction is screened and the transition moves to lower ω as the IB moves closer to the VB [5,18].

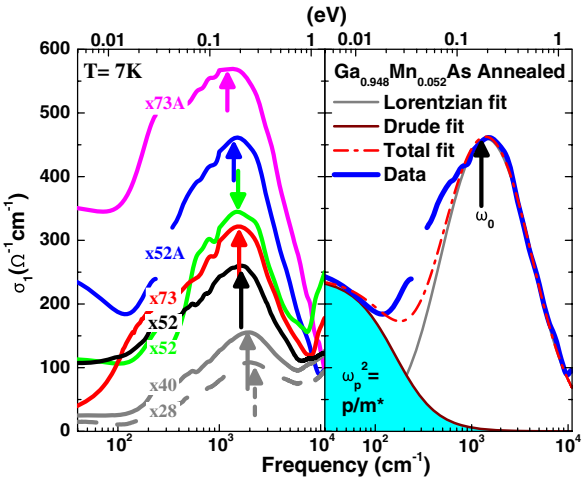

FIG. 1 (color online). The real part of the conductivity for all samples in this study as well as the results of previous studies (black and gray lines) [8]. A clear increase in $\sigma_1(\omega)$ is seen as the result of larger x and/or annealing. Right side: The results of fitting the 52A data with the two-component model [Eq. (1)].

To investigate these scenarios, we examined the position of the MIR resonance in the conductivity data (ω_0) using two complimentary methods. First, we looked for the maximum in $\sigma_1(\omega, x)$ by setting $\frac{d\sigma_1(\omega,x)}{d\omega} = 0$. In addition, we have fit the data presented in Fig. 1 with the two-component model of Eq. (1) and obtained ω_0 from the

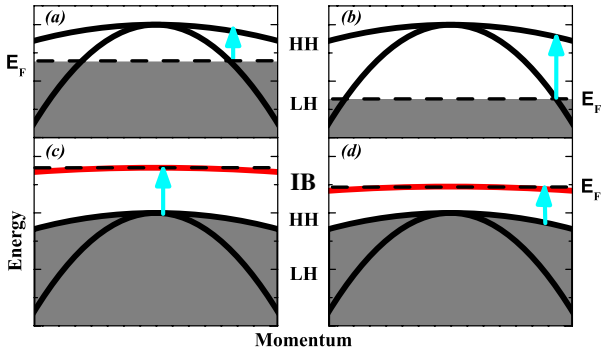

FIG. 2 (color online). Two scenarios for the electronic structure of $Ga_{1-x}Mn_xAs$ that have different implications for the resonant frequency of the MIR interband absorption. (a) E_F lies in the light and heavy hole (LH and HH, respectively) bands at low x, producing a transition between the two. (b) As p is increased, E_F moves farther into the LH and HH bands, causing the transition to blueshift. (c) If E_F lies in the IB, then at low x a transition occurs from the VB to the IB. (d) At higher p, E_F moves deeper in the IB, causing the feature to redshift.

resonant energy in the second term of Eq. (1) [21]. The resulting center frequency of the interband transition is shown via the arrows in Fig. 1 and is plotted in Fig. 3 as a function of the effective optical spectral weight, which is a measure of p:

$$N_{\mathrm{eff}}(\omega_c, x, T) = \frac{2}{\pi e^2}\int_0^{\omega_c} \sigma_1(\omega, x, T)d\omega \propto \frac{p}{m_{\mathrm{opt}}}, \quad (2)$$

with $\omega_c = 6450\ \mathrm{cm}^{-1}$. This cutoff was chosen to provide a direct connection to the theoretical calculations of the optical properties, in particular, the spectral weight of $Ga_{1-x}Mn_xAs$ [2]. We have found that the increase in spectral weight from sample to sample is mostly independent of ω_c; therefore the qualitative behavior shown in Fig. 3 is not effected by the choice of cutoff. Finally, the results from setting $\frac{d\sigma_1(\omega,x)}{d\omega} = 0$ and fitting the spectra using Eq. (1) are in good quantitative agreement.

The data in Fig. 3 demonstrate a rapid redshift of the MIR feature with an increase in p as quantified via the magnitude of N_{eff}. Eventually ω_0 levels off at approximately 1350 cm^{-1}. It is important to contrast these results with what has been seen in an optical study of the p-type GaAs doped to similar levels, where E_F clearly lies in the GaAs VB. In the latter system the inter-VB transitions clearly blueshift with the increase of p [17]. The same qualitative trend is obtained in a recent theoretical work [2] aimed at the analysis of inter-VB absorption in $Ga_{1-x}Mn_xAs$ (see right panel of Fig. 3). The position of the resonance plotted in this panel has been inferred from the model results for the conductivity by the $\frac{d\sigma_1(\omega,x)}{d\omega}$ method. Therefore our observation of redshifting of ω_0 is in direct contradiction to both experimental results and theoretical modeling of the optical response due to E_F situated in the VB of GaAs. Furthermore, the prediction of Ref. [2] for the magnitude of ω_0 is too high in energy to be consistent with our data.

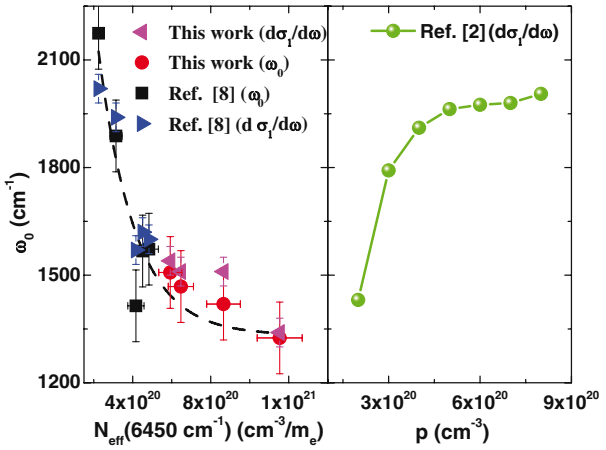

FIG. 3 (color online). Left panel: The peak position of the MIR feature determined by two alternative methods: setting $\frac{d\sigma_1(\omega,x)}{d\omega} = 0$ and from the two-component analysis. This is plotted versus the spectral weight below 6, 450 cm^{-1}, which is proportional to the number of holes [$N_{\mathrm{eff}}(6450\ \mathrm{cm}^{-1}) \propto p$]. This figure demonstrates that, regardless of the growth method, the MIR feature redshifts with increasing doping or p. Right panel: The results from the predicted behavior of the GaAs VB versus p for $x = 0.05$ [2], determined by the $\frac{d\sigma_1(\omega,x)}{d\omega}$ analysis [22].

Next we inquire into the nature of the states at E_F through the examination of the plasma frequency. Since we are able to separate out the free-carrier component in the annealed films, this analysis is particularly fruitful as we can estimate the effective mass of the holes: $m^* \propto \frac{p}{\omega_p^2}$. Previous optical studies of p-type GaAs where E_F lies in the VB have demonstrated that $m^* = 0.38m_e$ [17]. Assuming between 0% and 50% compensation of the Mn for the annealed samples, we find the effective mass to be of the order of $10m_e$; however, the precise value depends on an accurate account of the degree of compensation. Furthermore, theoretical calculations suggest that if E_F lies in the VB, then an optical mass ($m^{\mathrm{opt}} \propto \frac{p}{N_{\mathrm{eff}}(800\ \mathrm{meV})}$) should be independent of p and lie between $0.25m_e \rightarrow 0.29m_e$ [2]. Using the same assumptions for p we find $0.7m_e < m^{\mathrm{opt}} < 1.4m_e$ for both the 52A and 73A films. The m^* reported here likely reflect strong interactions in $Ga_{1-x}Mn_xAs$, yet the carriers are still too heavy for E_F to lie in the GaAs VB.

Since it is well established that the disorder in $Ga_{1-x}Mn_xAs$ is strong and is likely to become more significant as x is increased (due to the additional Mn_i that are introduced) [15], it is important to discuss what effects impurities may have on our results. One may be tempted to hypothesize that the redshifting results from the additional defects in the samples. However, annealing reduces the disorder and enhances the carrier density by removing Mn_i. In fact, our observation of a clear Drude feature only in annealed samples (see Fig. 1) confirms a *reduction* of scattering upon annealing the films. Nonetheless, the MIR feature continues to redshift after annealing, suggesting that disorder plays little to no role in its position. This is not surprising, since our discussion of the redshifting of ω_0 with p does not rely on k conservation, only on the energy difference between the center of the IB and the top of the VB. Furthermore, disorder generally broadens the observed width of optical transitions, but does not significantly affect their position. Finally, as discussed below, the clear observation of critical points in $Ga_{1-x}Mn_xAs$ [9,23] argues against disorder significantly effecting the optical properties of these samples.

The data in Figs. 1 and 3 provide conclusive evidence that the holes in $Ga_{1-x}Mn_xAs$ resides in a Mn-induced impurity band regardless of carrier density, thereby establishing the basic model of the electronic structure of this prototypical magnetic semiconductor. This conclusion has a number of interesting implications and raises some important new questions. First, unmistakable evidence for IB conduction in $Ga_{1-x}Mn_xAs$ suggests that heavy masses associated with states at E_F have to be taken into consideration in designing device functionalities involving spin

and/or charge injection as well as magneto-optical effects. Second, the large values of m^* we have found provides an explanation of the rather low mobility ($\mu = \frac{e\tau}{m^*}$) of $Ga_{1-x}Mn_xAs$. Intriguingly, even the cleanest samples of $Ga_{1-x}Mn_xAs$ demonstrating high values of T_C reveal μ as low as 1–5 $cm^2/V\,s$, which is 1 to 2 orders of magnitude smaller than in GaAs doped to similar concentrations with nonmagnetic impurities. In fact, to produce such low mobilities in III-V materials, one generally has to make the crystals amorphous. However, all films in this study reveal van Hove singularities via spectroscopic ellipsometry [9] and optical magneto circular dichroism (MCD) [23], indicating that the carrier momentum is still a good quantum number. One can also evaluate the strength of disorder via a calculation of the product of the mean free path (l) and Fermi momentum (k_F). Assuming a single band and the same values of p used for the extraction of the effective mass, in the annealed samples we find $3 < k_F l < 5$. Since these values are significantly larger than 1, they indicate that the transport in these samples is coherent. Therefore the low mobility of $Ga_{1-x}Mn_xAs$ cannot originate solely from low values of τ. Thus the low values of μ cannot be understood as simply arising from disorder, implying that heavy effective masses reported here are the primary cause of the small mobility in $Ga_{1-x}Mn_xAs$.

Interestingly recent optical and x-ray MCD studies [23] have suggested the exchange constant is rather large in $Ga_{1-x}Mn_xAs$, which may explain the significant enhancement of $\frac{m^*}{m_e}$ that we observe. Specifically it has been shown by numerous authors that large values of the exchange will tend to localize the holes around the Mn [1,4,5]. Furthermore, the localization effect described above may also account for the persistence of the IB in annealed $Ga_{1-x}Mn_xAs$ [4,5]. Nonetheless, the existence of the IB presents a significant challenge to our current conception of the MIT in doped semiconductors. In particular, it is a long held belief that the IB that emerges at low doping levels is built purely from hydrogenic states of the acceptor, and therefore can never produce Bloch waves. The metallic transport in doped semiconductors is then understood via the assumption that once the Coulomb attraction between the holes and the acceptors is completely screened the IB "dissolves" into the main band. This then implies that the holes now occupy Bloch states, resulting in metallic behavior. Our results suggest that this picture is incomplete when doping is accomplished with magnetic impurities. Interestingly recent tight-binding calculations suggest a Mn-induced resonance in the VB, which may account for our results [6]. Specifically, while our results require the presence of an IB, they cannot exclude its overlap with the VB in the density of states. Clearly further studies are needed to clarify the interplay between the carrier dynamics, band structure, and ferromagnetism of $Ga_{1-x}Mn_xAs$.

The work at UCSD was supported by the DOE and NSF, and the work at UCSB and PSU was supported by DARPA and ONR. We are grateful for our discussions with L. Cywinski, M. E. Flatte, A. MacDonald, A. J. Millis, S. Das Sarma, J. Sinova, J.-M. Tang, and C. Timm.

*Permanent address: Los Alamos National Laboratory, MS G756, MST-CINT, Los Alamos, NM 87545, USA. Electronic address: kburch@lanl.gov

†Permanent address: Department of Physics, California State University, East Bay, CA 94542, USA.

‡Permanent address: Department of Physics, University of California, Riverside, CA 92521, USA

[1] A. H. MacDonald *et al.*, Nat. Mater. **4**, 195 (2005).
[2] J. Sinova *et al.*, Phys. Rev. B **66**, 041202 (2002).
[3] B. Lee *et al.*, Semicond. Sci. Technol. **17**, 393 (2002); T. Dietl *et al.*, Science **287**, 1019 (2000).
[4] M. Berciu and R. N. Bhatt, Phys. Rev. B **69**, 045202 (2004); G. Alvarez and E. Dagotto, Phys. Rev. B **68**, 045202 (2003); S. Sanvito *et al.*, Phys. Rev. B **63**, 165206 (2001); S. C. Erwin and A. G. Petukhov, Phys. Rev. Lett. **89**, 227201 (2002); P. Mahadevan and A. Zunger, Phys. Rev. B **69**, 115211 (2004); M. A. Majidi *et al.*, cond-mat/0510716.
[5] E. H. Hwang *et al.*, Phys. Rev. B **65**, 233206 (2002).
[6] J. M. Tang *et al.*, Phys. Rev. Lett. **92**, 047201 (2004).
[7] J. Moreno *et al.*, Phys. Rev. Lett. **96**, 237204 (2006).
[8] E. J. Singley *et al.*, Phys. Rev. Lett. **89**, 097203 (2002); Phys. Rev. B **68**, 165204 (2003).
[9] K. S. Burch *et al.*, Phys. Rev. B **70**, 205208 (2004).
[10] K. S. Burch *et al.*, Phys. Rev. B **71**, 125340 (2005).
[11] O. Rader *et al.*, Phys. Rev. B **69**, 075202 (2004); J. Okabayashi *et al.*, Physica (Amsterdam) **10E**, 192 (2001).
[12] V. F. Sapega *et al.*, Phys. Rev. Lett. **94**, 137401 (2005).
[13] S. J. Potashnik *et al.*, Appl. Phys. Lett. **79**, 1495 (2001).
[14] K. W. Edmonds *et al.*, Appl. Phys. Lett. **81**, 3010 (2002); T. Hayashi *et al.*, Appl. Phys. Lett. **78**, 1691 (2001).
[15] K. W. Edmonds *et al.*, Phys. Rev. Lett. **92**, 037201 (2004); K. M. Yu *et al.*, Phys. Rev. B **65**, 201303(R) (2002).
[16] M. B. Stone *et al.*, Appl. Phys. Lett. **83**, 4568 (2003); W. Limmer *et al.*, Phys. Rev. B **71**, 205213 (2005); V. Stanciu *et al.*, Phys. Rev. B **72**, 125324 (2005).
[17] W. Songprakob *et al.*, J. Appl. Phys. **91**, 171 (2002).
[18] S. Liu *et al.*, Phys. Rev. B **48**, 11 394 (1993).
[19] D. N. Basov *et al.*, Europhys. Lett. **57**, 240 (2002).
[20] We note that this sum rule assumes that the free-carrier response is separated from the interband response, and that the cutoff (Ω) is chosen to be many times Γ_D.
[21] We set $\sigma_{dc} = \sigma(30\ cm^{-1})$ to reduce the number of fit parameters.
[22] Fitting the results of Ref. [2] with the two-component model indicates that their ω_0 is approximately 500 cm^{-1} greater than that displayed with green dots in the right panel of Fig. 3.
[23] D. J. Keavney *et al.*, Phys. Rev. Lett. **91**, 187203 (2003); K. Ando *et al.*, J. Appl. Phys. **83**, 6548 (1998); B. Beschoten *et al.*, Phys. Rev. Lett. **83**, 3073 (1999).